Available online at www.sciencedirect.com

ScienceDirect

Procedia Manufacturing 47 (2020) 1154–1158

Procedia MANUFACTURING

www.elsevier.com/locate/procedia

23rd International Conference on Material Forming (ESAFORM 2020)

Laser Metal Deposition of Ti-6Al-4V with a Direct Diode Laser Set-up and Coaxial Material Feed

Frank Silze[a], Michael Schnick[a], Irina Sizova[b,*], Markus Bambach[b]

[a]OSCAR PLT GmbH, Hamburger Ring 11, 01665 Klipphausen, Germany
[b]Chair of Mechanical Design and Manufacturing, Brandenburg University of Technology Cottbus - Senftenberg, Konrad - Wachsmann - Allee 17, 03046 Cottbus, Germany

* Corresponding author. Tel.: +49-355-69-3431; fax: +49-355-69-3110. *E-mail address:* sizova@b-tu.de

Abstract

The production of components from the titanium alloy Ti-6Al-4V is of great importance for many industrial fields, especially for the aerospace industry. Laser metal deposition (LMD) processes can be used either for manufacturing of components or repair. The majority of LMD set-ups use a concentrical laser and a powder feed through nozzles focusing the powder on a spot. Gas shielding is problematic in such set-ups, which hence require the use of protective gas chambers. The present paper details results on laser metal deposition (LMD) of Ti-6Al-4V with a new direct diode laser head. In the LMD set-up, six 200W laser diodes are positioned on a circle around the feeding lance and create a laser spot with a diameter of ~0.9 mm. The laser beam is thus directly generated inside the head. The set-up allows for co-axial feed of powder or wire material. Due to the arrangement of the single laser beams and the coaxial filler material feeding, a direction independent welding process is possible. The Ti-6Al-4V specimens deposited with the LMD head show a clean surface and a dense microstructure. The results indicate that the new diode laser head allows for a direction-independent LMD process with low oxygen take-up.

Keywords: Laser Metal Deposition; Ti-6Al-4V; Aerospace

1. Introduction

Surface coating, repair of high-performance components, such as jet-engine parts and generating complex structures are challenging applications for laser metal deposition technologies [1, 2]. Unlike powder bed technologies such as selective laser melting (SLM), which shows its benefits in the production of rather small but complex-shaped parts [3], the laser metal deposition (LMD) may be used to produce larger components, to deposit claddings with very low weld penetration, and to add specific features on conventionally produced parts.

Especially the last point makes LMD interesting for hybrid production processes. LMD can be used for the production of complex components, where the required features, i.e. cooling or reinforcement ribs or other structural or functional elements can be added to the conventionally manufactured workpiece. Avoiding the extensive use of machining and thus reducing the amount of scrap may lead to lower costs of production.

However, the direction-dependence of the LMD process inherent especially in many wire-feed process set-ups is an important aspect of process planning and component performance. In the present work, a newly developed LMD head is used, which consists of a diode laser system with six laser diodes arranged on a circle. Due to the arrangement of the single laser beams a coaxial feed of filler material is possible and a direction independent welding process is achieved this way. Powder, wire and hot wire can be used in a single set-up. The LMD head is particularly interesting for hard to handle high-performance materials. In the previous work of the authors, it was shown that using this laser head with the coaxial filler material feeding workpieces of Inconel

10.1016/j.promfg.2020.04.156

718 with a homogeneous structure and a defect-free microstructure can be produced [4]. This process can also be applied to titanium alloys. Ti-6Al-4V is the most commonly used titanium alloy in the aerospace industry today due to its high strength-to-weight ratio, moderate ductility, good fatigue behavior, high fracture resistance and excellent corrosion properties. Mechanical properties of Ti-6Al-4V are related to its microstructural morphology [5]. The components produced by LMD often represent complex microstructures varying spatially within the deposited volume. The microstructure of Ti-6Al-4V manufactured by LMD is very sensitive to the thermal history. A martensitic or Widmanstätten-type microstructure is often found. Sometimes, grain boundary α-phase is present, depending on the cooling rates and peak temperatures during the manufacturing process. Moreover, an undesirable feature of LMD of Ti-6Al-4V is the formation of coarse-columnar primary ß-grain structures with an associated strong solidification texture and the grain boundary α-phase. The ß-grain sizes are mainly determined by the time the material is exposed to temperatures above the β-transus temperature [6]. The texture results from the solidification conditions in a heated moving melt pool, which promotes a high thermal gradient at the solidification front [7]. The study of Baufeld et al. [6] showed that the grain sizes and the presence of detrimental grain boundary α-phase depend strongly on the heat input and the cooling rate in the LMD process, i.e., deposition processes with lower heat input and higher cooling rates produce smaller β grain sizes and thinner lamellae, and consequently better material properties. One possibility to induce higher cooling rates is the application of increased interlayer dwell times. Foster et al. [8] reported that increasing interlayer dwell time results in a slight decrease in the α lath width and a much more noticeable decrease in the width of prior-β grains during wire-arc additive manufacturing (WAAM) of Ti-6Al-4V. Zhao et al. [9] showed that both interlayer stress and residual stress can be reduced by controlling interlayer cooling time during additive manufacturing. However, the interlayer cooling time decreases the production rate and a compromise should be found for optimum process parameters which also provide improved mechanical properties.

The purpose of the present study is to establish an LMD wire process and to investigate the influence of variations of the interlayer dwell time on the related changes in microstructure. The paper is structured as follows: Section 2 gives an overview of the manufacturing of the samples from Ti-6Al-4V using the coaxial direct diode laser head with different dwell times. Also, the procedures of microstructural analysis are presented. Section 3 details the results and discussion of metallographic examinations. Finally, conclusions and outlook are presented.

2. Materials and methods

The LMD process was performed with a 1.2 kW direct diode laser head (Fig. 1) which was mounted on a Fanuc 6-axis robot (Fig. 2). Argon shielding gas was used to prevent the oxidation of the material. A beam transport fiber is not needed in this set-up. Only current and cooling water need to be connected to the LMD head. The filler metal in the form of wire can easily be fed perpendicular to the substrate surface into the laser spot.

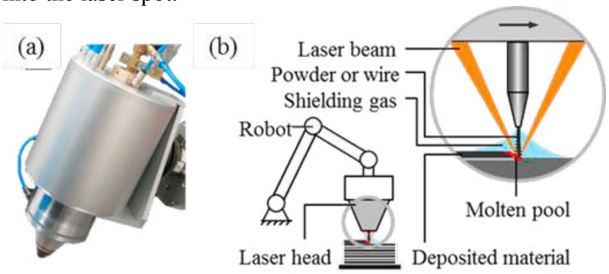

Fig. 1. (a) Close-up of the laser head and (b) schematic of the coaxial laser beam and feeding lance arrangement.

Fig. 2. Experimental set-up with trial specimens.

The most widely used titanium alloy Ti–6Al–4V was selected for the investigations in the present study. The geometry used in the current study represents a wall with a length of 98 mm and a width of 12 mm. Using LMD the walls were manufactured to a total height of 100 mm (s. Fig. 3). Ti-6Al-4V wire with a diameter of 1 mm was used. The wire was deposited on Ti-6Al-4V plates with a thickness of 12 mm. All substrate surfaces were cleaned prior to the welding process using acetone.

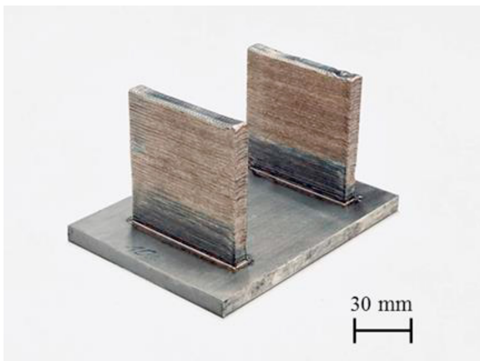

Fig. 3. Geometry of the walls manufactured by LMD.

A bidirectional scanning strategy with a rotation of 90° of the scanning direction was chosen for the manufacturing of the walls and is schematically represented in Fig. 4. The distance between parallel track lines was defined as the hatch distance and was approximately 1.3 mm. The layer thickness was 1.3 mm. An overlap of 52% of the nominal track width was chosen in order to ensure the formation of continuous and proper bonding between successive tracks. This value was determined experimentally in a preliminary study. The process parameters like laser power, scanning speed, the resulting linear energy input and the wire feed rate are listed in Table 1.

Table 1. Parameter setup of the deposition processes with Ti-6Al-4V wire.

Spot size, mm	Laser Power, W	Scan Speed, mm/s	Energy input, J/mm	Feed rate, m/min
0.9	1000	14.5	69	0.98

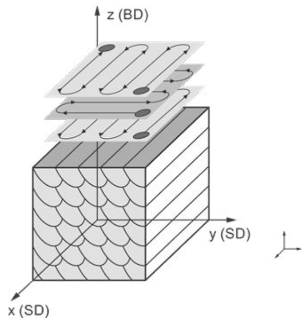

Fig. 4. Schematic illustration of the scanning strategy.

After the deposition of each layer, different interlayer dwell times were applied. The interlayer dwell time allows for cooling and for moving the LMD head back for the start of the next deposition pass. The total deposition time per layer was 40 seconds, and the total interlayer dwell time was varied from 1 to 20 seconds. Samples for the analysis of microstructure were cut along the building direction. The samples were mounted with cut cross-sections on top and ground flat with successively finer grades of silicon carbide (SiC) papers from 320 to 1200. The specimens were then polished with 0.05 µm silica solution (Struers OP-S Suspension) with the addition of H_2O_2, HNO_3, and HF. Kroll's agent etching was used to reveal the microstructure.

3. Results and discussion

3.1. Microstructure evolution

For all the deposited walls obtained with four different interlayer dwell times, no apparent defects between the substrate and the first layer of the deposit were observed indicating a sound metallurgical bonding in the transition zone. Also, the deposited material shows a microstructure without defects with only single small voids (less than 10 µm).

It was expected that changes in dwell time would impact the microstructures in Ti-6Al-4V walls manufactured by LMD. Microstructures of the walls produced with different dwell times show differences in the α-lath thickness and prior β-grain sizes as well as the thickness of the α-grain boundary layers. The corresponding microstructures produced in the Ti-6Al-4V deposited walls with 1, 5, 10 and 20-seconds interlayer dwell times are shown in Figures 5 and 6, respectively. The presented areas were located on cross-sections parallel to the building direction, in the center of manufactured walls (approximately 50 mm from the substrate). These areas were chosen to keep the influence of phase transitions caused by the additional cooling by the cold substrate (the layers in the bottom) and the effect of extremely fast cooling (the layers in the top) as small as possible.

The microstructures of all manufactured Ti-6Al-4V walls are characterized by epitaxial growth of large columnar prior β-grains which stretch through the deposited layers. Grain boundaries from the large columnar prior β-grains are also visible and are aligned almost perpendicular to the surface of the substrate (Fig. 5). Also, all walls appeared to have similar microstructural features that include a randomly oriented α - 'basket weave' microstructure within the columnar prior β-grains. Such structures developed due to the repeated rapid heating and cooling that occurs during the LMD process.

As was mentioned above, the different interlayer dwell times result in different cooling rates. An increase of cooling rate, i.e., increase of cooling time between layers, leads to the formation of thinner α-platelets, smaller β-grains, and reduced the thickness of α-grain boundary phase.

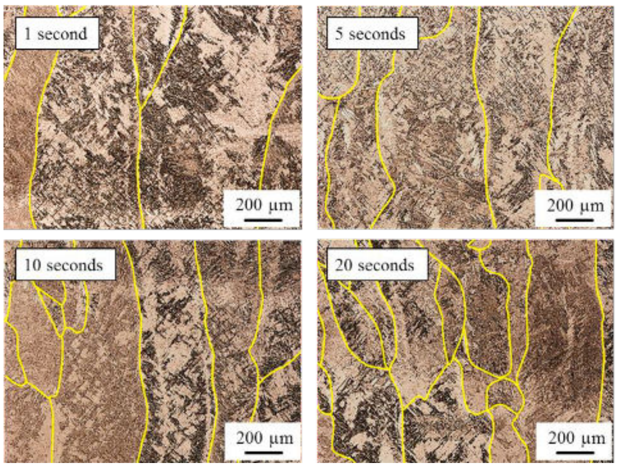

Fig. 5. Macrostructure images of LMD Ti-6Al-4V walls produced with different dwell times (β-grain boundaries are shown with lines).

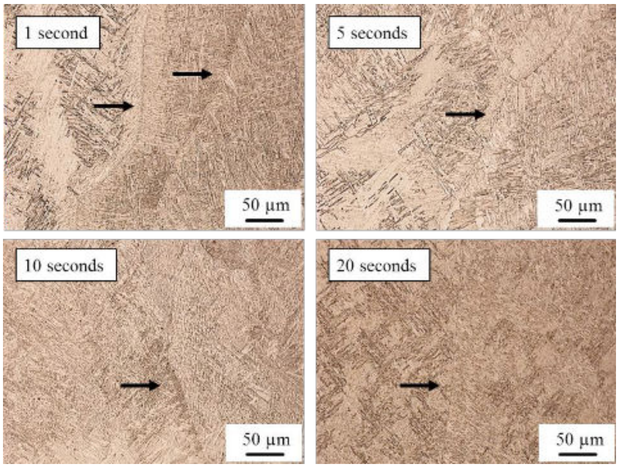

Fig. 6. Microstructure images of LMD Ti-6Al-4V walls produced with different dwell times (the boundaries of prior β-grains are shown with arrows).

In Table 2, an overview of the microstructural features for all four walls is presented. As can be seen, with the increase of interlayer dwell time to 20 s the thickness of α-platelets can be reduced to 1.5 µm, compared to 1.8 µm in the wall with an interlayer dwell time of 1 s. Also, the average width of β-grains is almost half of the width found in the wall produced with an interlayer dwell time of 1 s (450 µm at 20 s compared to 860 µm at 1 s). It should be marked, that by increasing interlayer dwell time to 20 s the thickness of the α-grain boundary phase is reduced to 1.2 µm, which could be beneficial for the mechanical properties.

Table 2: Overview of microstructural features of the walls produced with different interlayer dwell times.

Dwell time, s	α-thickness, µm	β-grain sizes, µm	α-grain boundary, µm
1	1.8	860 x 7370	2.2
5	1.8	750 x 7160	2.0
10	1.7	600 x 6450	1.9
20	1.5	450 x 5390	1.2

To understand the influence of dwell time on mechanical properties preliminary tensile tests were performed. Round tensile specimens were extracted perpendicular to the build direction from all walls, using wire EDM machining. The round tensile specimens M8 had a dog-bone shape with a gauge length of 25 mm and a diameter of 5 mm. Tensile testing was performed using an Instron model 4202 test frame with a 10 kN load cell (Instron model 2512-147). The specimens were tested at a constant loading rate and the strain rate averaged 0.002 s^{-1}.

In accordance with specifications for the aerospace industry, stress relief annealing should be performed after welding. Thus, before the investigation of mechanical properties, all walls were heat-treated at a temperature of about 710 °C for 2 hours and cooled in air. Generally, stress-relieving treatment decreases undesirable residual stresses that result from the LMD process without adversely affecting strength or ductility as well as microstructure. The results from the tensile testing are summarized in Table 3.

Table 3. Comparison of yield strength, tensile strength, and elongation at failure for samples produced with different dwell times.

Dwell time, s	YS, MPa	UTS, MPa	A5, %
1	949	1007	9.0
5	999	1060	7.5
10	977	1034	7.9
20	988	1044	9.7
ASTM B381-13	830	900	10

As can be seen, the tensile strength properties exceed the minimum tensile strength requirements of forged Ti-6Al-4V material, specified by ASTM B381-13 which are a yield stress (YS) of 830 MPa, and an ultimate tensile strength (UTS) of 900 MPa. However, the values of tensile elongation are slightly lower than required in the specification. Moreover, there is no consistent dependence of the tensile elongation of the material on the changes in the dwell times. For example, the samples from the wall produced with an interlayer dwell time of 1 s exhibit a higher elongation value (9.0 %) compared to 7.9 % at a dwell time of 10 s. Clearly, more repetitions of tensile tests are needed to estimate the variance of the results. At present, it seems that the mechanical properties are not only affected by the phases in the specimen and their morphology but also by oxygen take-up. This phenomenon was observed earlier [10, 11]. The obtained results are considered as preliminary and the investigation will be continued in order to analyze the microstructural transformations during LMD by adding different dwell times and their influence on the mechanical properties of the components. The effect of oxidation on the mechanical performance should be studied and measures seem necessary to avoid oxidation as much as possible.

4. Conclusion

In the present study, it was shown that Ti-6Al-4V walls can be produced with a clean surface and a dense microstructure using the new diode laser head. The effect of the interlayer dwell time on the related changes in microstructure was investigated. All deposited Ti-6Al-4V walls exhibit a 'basket weave' microstructure within the columnar prior β-grains. The different interlayer dwell times influence the microstructure. The results obtained in this work show that increasing dwell time allows for additional cooling during the deposition process and results in a reduced thickness of α-platelets, smaller β-grain sizes and leads to a visible decrease of the thickness of grain boundary α-phase. This can contribute to the improvement of mechanical properties of manufactured LMD components, e.g., to high tensile strength with adequate ductility.

Acknowledgments

The authors acknowledge funding through the DFG project BA4253/13-1 “Warmumform- und Schädigungsverhalten von additiv gefertigtem Ti6Al4V”. The authors are also grateful to the colleagues from the Chair of Physical Metallurgy and Materials Technology of BTU Cottbus-Senftenberg for the preparation of the micrographs shown in this study.

References

[1] Kaierle S, Barroi A, Noelke C, Hermsdorf J, Overmeyer L, Haferkamp H. Review on Laser Deposition Welding: From Micro to Macro. Phys. Procedia 2012;39:336–345.

[2] Gasser A. Fertigen und Instandsetzen mit generativenLaserverfahren. Maschinemarkt 2014;38:44–47

[3] Gu D, Meiners W, Wissenbach K, Poprawe R. Laser additive manu-facturing of metallic components: materials, processes and mechanisms. Int. Mater. Rev 2012; 57:133-164.

[4] Bambach M, Sizova I, Silze F, Schnick M. Hot workability and micro-structure evolution of the nickel-based superalloy Inconel 718 produced by laser metal deposition. J. Alloys Compd. 2018;740:278-287.

[5] Murr L, Gaytan S, Medina F, Martinez E, Martinez J, Hernandez D, Machado B, Ramirez D, Wicker R. Characterization of Ti-6Al-4V open cellular foams fabricated by Additive anufacturing using Electron Beam Melting. Mater. Sci. Eng., A 2010;527:1861-1868.

[6] Baufeld B, Brandl E, Van der Biest O. Wire based additive layer manufacturing: Comparison of microstructure and mechanical properties of Ti–6Al–4V components fabricated by laser-beam deposition and shaped metal deposition. J. Mater. Process. Technol. 2011;211:1146-1158.

[7] Qian L, Mei J, Liang J, Wu X. Influence of position and laser power on thermal history and microstructure of direct laser fabricated Ti–6Al–4V samples. Mater. Sci. Technol. 2005;21: 597-605

[8] Foster BK, Beese AM, Keist JS, McHale ET, Palmer TA. Impact of interlayer dwell time on microstructure and mechanical properties of nickel and titanium alloys. Metall. Mater. Trans. A 2017;48:4411-4422.

[9] Zhao H, Zhang G, Yin Z, Wu L. Effects of Interpass Idle Time on Thermal Stresses in Multipass Multilayer Weld-Based Rapid Prototyping, J. Manuf. Sci. Eng. 2013;135:011016-011016-6.

[10] De Formanoir C, Michotte S, Rigo O, Germain L, Godet S. Electron beam melted Ti–6Al–4V: Microstructure, texture and mechanical behavior of the as-built and heat-treated material. Mater. Sci. Eng., A 2016; 652:105-119.

[11] Li X, Xie J, Zhou Y. Effects of oxygen contamination in the argon shielding gas in laser welding of commercially pure titanium thin sheet. J. Mater. Sci. 2005;40:3437-3443